Materials Science & Engineering A 647 (2015) 241–248

Contents lists available at ScienceDirect

Materials Science & Engineering A

journal homepage: www.elsevier.com/locate/msea

Nanostructure evolution and mechanical property changes during aging of a super duplex stainless steel at 300 °C

Niklas Pettersson [a,*], Sten Wessman [a], Mattias Thuvander [b], Peter Hedström [c], Joakim Odqvist [c], Rachel F.A. Pettersson [d], Staffan Hertzman [e]

[a] Swerea KIMAB AB, P.O. Box 7047, SE-164 07 Kista, Sweden
[b] Department of Applied Physics Chalmers University of Technology, SE-412 96 Göteborg, Sweden
[c] Department of Material Science and Engineering, KTH Royal Institute of Technology, SE-100 44 Stockholm, Sweden
[d] The Swedish Steel Producers' Association, Box 1721, SE-111 87 Stockholm, Sweden
[e] Outokumpu Stainless Research Foundation, Brinellvägen 23, SE-100 44 Stockholm, Sweden

ARTICLE INFO

Article history:
Received 4 August 2015
Received in revised form
28 August 2015
Accepted 2 September 2015
Available online 7 September 2015

Keywords:
Duplex stainless steel
Spinodal decomposition
Phase separation
Mechanical properties
Atom probe tomography (APT)
Transmission electron microscopy (TEM)

ABSTRACT

The nanostructure evolution and the corresponding changes in mechanical properties of a super duplex stainless steel 2507 (UNS S32750) during aging at 300 °C up to 12,000 h have been investigated. Microstructural studies using transmission electron microscopy and atom probe tomography show that subtle Cr concentration fluctuations develop during aging. The amplitude of the concentration fluctuations is proportional to the hardness of the ferrite phase, and it is also proportional to the decrease in room temperature impact toughness during aging. The fracture behaviour of the alloy changes gradually from ductile to cleavage fracture, upon aging. The cracks were found to propagate through the ferrite phase, partly along deformation twin interfaces, and delamination between the austenite and ferrite phases was observed.

1. Introduction

Duplex stainless steels are a category of alloys that combines high strength with excellent corrosion resistance [1]. This attractive combination of properties derives from the mixed microstructure, which consists of approximately equal amounts of ferrite and austenite. The duplex stainless steels are, however, sensitive to aging embrittlement in certain temperature ranges. This prevents their use in load-bearing applications in which the material is exposed to elevated temperatures for prolonged times during service. Restrictions on the upper service temperature are found e.g. in boiler and pressure vessel design codes due to the increased risk for reduced toughness. For the super duplex stainless steel 2507 (UNS S32750) a maximum service temperature of 250 °C is recommended in the VdTÜV standard [2], the Pressure Equipment Directive for the European Union [3], and the ASME Boiler and Pressure Vessel Code [4].

The low-temperature embrittlement phenomenon, which is generally referred to as the 475 °C embrittlement, is a consequence of Fe and Cr immiscibility [5]. When exposed to temperatures within the Fe–Cr miscibility gap, ferrite can decompose into a nanostructure consisting of Fe-rich α and Cr-rich α' regions, either by nucleation and growth, or by spinodal decomposition [6]. The phase separation, which is fastest at temperatures around 475 °C causes gradual hardening of the ferrite phase and loss of toughness with increased aging time. Other mechanisms that could cause embrittlement of duplex stainless steels, such as interstitial segregation [7], substitutional solute clustering [8–10] and G-phase formation [11,12] have also been reported to occur in this temperature range.

There are several studies on the effects of phase separation on the mechanical properties of both single-phase ferritic [7,13] and duplex stainless steels [10,12,14,15]. However, the detailed relation between phase separation, hardening and fracture behaviour of duplex stainless steels is still not fully understood. The recent advances in materials characterization tools open up for quantitative assessment of the nanostructure evolution during phase separation, and consequently enable the delineation of the structure-property relation. Thus, the aim of the present work has been to study thoroughly the low-temperature embrittlement occurring in the super duplex stainless steel 2507. In the present work both atom probe tomography (APT) and analytical transmission electron microscopy (TEM) have been applied. The microstructural investigations are combined with evaluation of hardness and impact toughness as well as fractography studies using scanning

* Corresponding author.
E-mail address: niklas.pettersson@swerea.se (N. Pettersson).

http://dx.doi.org/10.1016/j.msea.2015.09.009
0921-5093/

electron microscopy (SEM) and electron backscatter diffraction (EBSD) to develop a more comprehensive understanding of the embrittlement phenomenon.

2. Experimental details

2.1. Material and heat treatment

Plate material of the super duplex stainless steel 2507, with thickness 6 mm, was delivered by Outokumpu Stainless AB. The chemical composition is given in Table 1 and a three-dimensional representation of the microstructure is shown in Fig. 1. Specimens of approximate dimensions 150 mm × 150 mm × 6 mm were subjected to isothermal aging at 300 °C for up to 12,000 h.

2.2. Mechanical testing

The impact toughness was evaluated at room temperature using sub-size Charpy V specimens with dimensions 55 mm × 10 mm × 5 mm. The specimens were machined from the aged plates with the long side transverse to the rolling direction, and the notch positioned in the through-thickness direction (T–L orientation). Four specimens were tested for each material condition.

Vickers micro-hardness measurements on the austenite and ferrite phases were performed on the transverse section using a Qness Q10 micro-hardness tester and a 5 g load (HV0.005). Prior to hardness measurements, the samples were polished to 0.25 μm diamond finish and lightly etched in a solution of 100 ml HCl, 10 ml HNO_3 and 100 ml H_2O. At least 15 indentations were made in each phase.

2.3. Atom probe tomography

The APT analyses were performed using a LEAP 3000X HR (Imago Scientific Instruments). The specimen temperature was set to 40 K, the pulse fraction was 20%, the pulse frequency 200 kHz and the detection rate 0.5%. The reconstructions were made using an evaporation field of 33 V/nm and a *k*-factor of 3.8, in the software IVAS 3.4.4 (Cameca). Samples for APT were prepared by the standard two-step electropolishing procedure. About half of the analyses contained austenite and half contained ferrite (random positioning). The phases could easily be identified since the ferrite contains virtually no C, while the MoN-peaks are higher than the Mo-peaks in the mass spectrum from analysis of austenite.

A sensitive method for evaluating spinodal decomposition is to use the radial distribution function (RDF) [16]. In order to construct an RDF for Cr, the radial concentration profile starting from each individual Cr atom is calculated. The datasets used here contained about 9 million atoms, i.e. about 2 million Cr atoms. Hence, the RDF is the sum of about 2 million concentration profiles. As Cr is slightly enriched in some areas (the α'-phase), the resulting RDF (Cr concentration profile around Cr atoms) will show higher values at short distances because a majority of the profiles starts in Cr-rich regions. Here, bulk normalized RDFs have been used (showing the concentration profile divided by the measured average Cr concentration). Some regions around certain crystallographic poles were removed before constructing RDFs [17].

Table 1
Chemical composition in wt%, of 2507 (UNS S32750) from the plate certificate.

C	Si	Mn	P	S	Cr	Ni	Mo	N	Cu
0.012	0.30	0.83	0.023	0.001	24.84	6.90	3.80	0.28	0.18

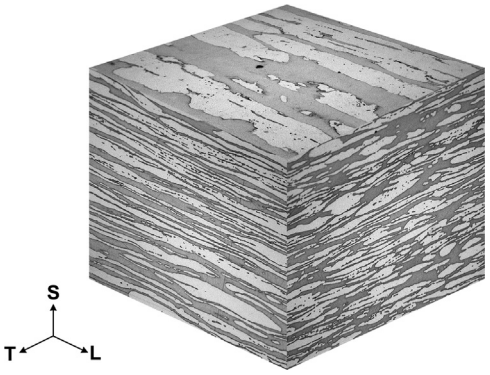

Fig. 1. Three-dimensional microstructure of super duplex 2507 in as-delivered condition with austenite etched bright and ferrite dark (each side is 210 μm × 210 μm).

The overlap of $^{54}Cr^{2+}$ and $^{54}Fe^{2+}$ in the mass spectra was deconvoluted using the natural isotope abundance when evaluating the phase composition, but for statistical analyses this peak was instead omitted.

In order to divide the analyses of ferrite into α and α' phases, iso-concentration surfaces were constructed using a voxel size of 1 nm^3 and delocalization distances of 3 nm × 1.5 nm × 1.5 nm.

The amplitude of decomposition was evaluated from the RDF at zero distance (RDF_0, determined by fitting the RDF (0–2 nm) with a polynomial function of degree 4) and the theoretical RDF given by a one dimensional sinusoidal concentration profile ($A = C_0\sqrt{2(RDF_0 - 1)}$) [16].

2.4. Scanning electron microscopy

Fracture surfaces from impact toughness tests were imaged using a JEOL 7001F field emission gun (FEG) microscope. EBSD analysis of a fracture surface cross-section was performed using a Zeiss Supra 55 FEG-SEM equipped with a Nordlys^2 F+ camera. The software AZtechHKL and CHANNEL5 were used for acquisition and post-processing. Samples for EBSD analysis were prepared by polishing with colloidal silica solution as the final step.

2.5. Transmission electron microscopy

Thin foils were prepared by electrolytic polishing at 12 V in a twin-jet polisher using an electrolyte consisting of 15% perchloric acid in methanol kept at −18 °C. TEM analyses were performed using a JEOL 2100F 200 kV FEG-TEM equipped with a high-angle annular dark-field (HAADF) detector and a Gatan Tridem post-column energy filter for electron energy loss spectroscopy (EELS) and energy-filtered imaging (EFTEM). HAADF imaging was performed in scanning beam mode (STEM). The thin foils were argon ion-beam polished in a Gatan precision ion polishing system prior to analysis.

3. Results

3.1. Mechanical properties and fracture behaviour

Results from impact toughness and hardness tests after aging for 3000, 6000 and 12,000 h at 300 °C are presented in Fig. 2. The aging time had a clear effect on the mechanical properties. There is a gradual loss in impact toughness from the unaged material down to 44% of the initial impact energy after 12,000 h of aging. At the same time the ferrite hardness increased by 56%, while no significant change in hardness could be detected for the austenite.

Fracture surfaces from the impact toughness tests are shown in Fig. 3. The unaged material displayed a ductile fracture surface